Frontiers of Information Technology & Electronic Engineering
www.jzus.zju.edu.cn; engineering.cae.cn; www.springerlink.com
ISSN 2095-9184 (print); ISSN 2095-9230 (online)
E-mail: jzus@zju.edu.cn

Fall preventive gait trajectory planning of a lower limb rehabilitation exoskeleton based on capture point theory*

Mei-ying DENG[1], Zhang-yi MA[2], Ying-nan WANG[2], Han-song WANG[2], Yi-bing ZHAO[2], Qian-xiao WEI[2], Wei YANG[2], Can-jun YANG[†‡2]

[1]*Zhejiang University Hospital, Hangzhou 310027, China*

[2]*State Key Laboratory of Fluid Power and Mechatronic Systems, Zhejiang University, Hangzhou 310027, China*

[†]E-mail: ycj@zju.edu.cn

Received Dec. 13, 2018; Revision accepted July 8, 2019; Crosschecked Oct. 10, 2019

Abstract: We study the balance problem caused by forward leaning of the wearer's upper body during rehabilitation training with a lower limb rehabilitation exoskeleton. The instantaneous capture point is obtained by modeling the human-exoskeleton system and using the capture point theory. By comparing the stability region with instantaneous capture points of different gait phases, the balancing characteristics of different gait phases and changes to the equilibrium state in the gait process are analyzed. Based on a model of the human-exoskeleton system and the condition of balance of different phases, a trajectory correction strategy is proposed for the instability of the human-exoskeleton system caused by forward leaning of the wearer's upper body. Finally, the reliability of the trajectory correction strategy is verified by carrying out experiments on the Zhejiang University Lower Extremity Exoskeleton. The proposed trajectory correction strategy can respond to forward leaning of the upper body in a timely manner. Additionally, in the process of the center of gravity transferred from a double-support phase to a single-support phase, the ratio of gait cycle to zero moment point transfer is reduced correspondingly, and the gait stability is improved.

Key words: Lower extremity exoskeleton; Capture point; Gait phase; Balance of human-machine system
https://doi.org/10.1631/FITEE.1800777 **CLC number:** TP242

1 Introduction

For patients with hemiplegia or paraplegia, which can be caused by a stroke or other cardiovascular and cerebrovascular diseases, early rehabilitation training is an important factor for their successful recovery. Lower limb exoskeletons have great potential for improving walking rehabilitation training, because they can guide the patients through repetitive, stable, and quantifiable movements, and provide various training modes and scenarios.

The balance of a lower limb rehabilitation exoskeleton is of great significance to ensure the safety of patients. In the field of lower limb rehabilitation exoskeletons, extensive research on the balance problem has been conducted.

The most widely applied methods are to use crutches or other assistant devices to share part of the patient's bodyweight. Meanwhile, sole pressure and electromyography (EMG) signals are used to identify motional intentions of the human body to improve the balance ability of the human-exoskeleton system (Kyeong et al., 2019). For example, a hybrid auxiliary limb (HAL) monitors EMG signals (Kawamoto and Sankai, 2005), ReWalk measures the tilt angle of the upper body, and Ekso uses accelerometer sensors on crutches and pressure sensors on shoes to detect the walking intentions of the wearer (Strausser and Kazerooni, 2011). However, these methods are undesirable, because they rely on the aid of crutches and lack the capability of timely response to emergencies.

‡ Corresponding author

* Project supported by the National Natural Science Foundation of China (No. 51805469)

ORCID: Can-jun YANG, http://orcid.org/0000-0002-3712-0538

Another method is to use the zero moment point (ZMP) (Vukobratović and Stepanenko, 1973) and related concepts to control and judge the stability of the exoskeleton. Aphiratsakun et al. (2012) used the ZMP theory to control the gait of the ALEX exoskeleton, and Jatsun et al. (2016) used the ZMP theory and an iterative quadratic regulator to program the trajectory of an exoskeleton. However, these approaches do not take external effects of the human-exoskeleton systems into consideration.

Some researchers have attempted to change the physical structure of the exoskeleton system. The robot leg, supernumerary robotic limb (SRL), has not been designed to directly connect the lower limbs of the exoskeleton to the lower limbs of the wearer (Parietti et al., 2016). In Li et al. (2015), a pair of additional lower limb mechanisms has been added to the exoskeleton. Both of the two designs form new support areas with the human body, by adjusting the landing position of the lower limb exoskeleton/assistant mechanism, to solve the balance problem of the human-machine system. However, both of the two balance systems require good athletic ability and muscle power, which increases the complexity of the exoskeleton. Moreover, the extra lower limbs increase the volume and weight of the exoskeleton, which has adverse effect on the use of lower limb exoskeleton.

The center of mass (CoM) and its related theories have been taken into consideration by some researchers. Wang et al. (2015) analyzed the balance control of a human-exoskeleton system based on the concept of extrapolated CoM (XCoM), and designed a corresponding hip joint system to adjust the balance of the human-exoskeleton system by controlling the adduction/abduction of the hip joint.

Overall, human-exoskeleton systems are similar to the humanoid robot systems. Therefore, the approaches used to solve the balance problem in the field of humanoid robots should have a good chance of being successfully applied to human-exoskeleton systems. Currently, three kinds of balance recovery strategies are mostly adopted for humanoid robots: ankle/hip strategy, loading/unloading balance strategy, and stepping strategy.

There are two challenges of human-exoskeleton systems: the lack of movement ability of the wearer and the difference of movement ability among bilateral limbs. These can lead to a mismatch between the movements of the wearer and the lower limb exoskeleton, resulting in the forward leaning of the upper body and the declination of stability in the process of the center of gravity transfers during walking training. Considering the actual needs of a lower limb rehabilitation exoskeleton, and drawing lessons from the balance control strategies of humanoid robots, the stepping strategy is considered as a method that can solve the balance problem of human-exoskeleton systems. The balance of the human-exoskeleton system was studied using the capture point (CP) theory (Koolen et al., 2012).

2 Balance problem of human-exoskeleton systems

2.1 Linear inverted pendulum model plus flywheel system

In a lower limb rehabilitation exoskeleton, the human-exoskeleton system can be simplified as an equivalent flywheel and a left/right two-bar model with variable length (Fig. 1). According to the actual movement of the exoskeleton, in the single-support state, legs can be classified as the supporting and non-supporting legs. The supporting leg plays the major supporting role, while the non-supporting leg provides either a small contribution (such as that in the late supporting phase) or almost no contribution at all (such as that in the swing phase). The different supporting states or different moving phases will be described in detail in Section 2.2.

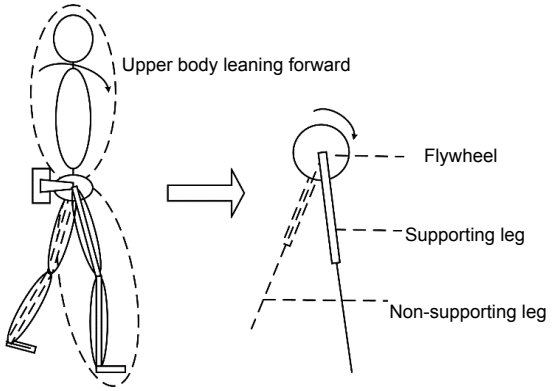

Fig. 1 Simplified model of the human-exoskeleton system

Because the non-supporting leg contributes less to the balance of the system, it can be transformed into an ideal model—the inverted pendulum system

of a flywheel composed of an equivalent flywheel and a supporting leg. In the actual walking process, the center of gravity of the human body has a fluctuation of 5 cm, which is relatively negligible compared with the height of the CoM.

Based on this, the supporting leg is simulated with a variable length and an axial internal force (f_l) in this model. Thus, a linear inverted pendulum model (LIPM) plus flywheel system is established for a single-support state (Fig. 2).

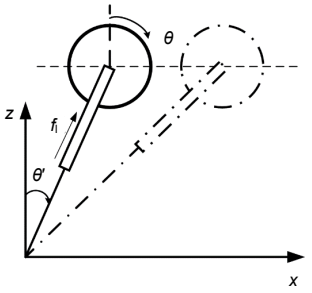

Fig. 2 Linear inverted pendulum model (LIPM) plus flywheel system

The dynamic analysis of this model is expressed as

$$m\ddot{x} = f_l \sin\theta' - \frac{J\ddot{\theta}}{l}\cos\theta', \tag{1}$$

$$m\ddot{z} = -mg + f_l \cos\theta' - \frac{J\ddot{\theta}}{l}\sin\theta', \tag{2}$$

where x and z represent location parameters of the equivalent flywheel, l the equivalent length of the pendulum, m and J the mass and inertia of the flywheel respectively, θ' and θ the angles relative to the z axis, f_l the bar force, and g the gravitational acceleration constant (Pratt et al., 2006; Englsberger et al., 2011).

Considering that θ' is a small angle, the trigonometric functions in Eqs. (1) and (2) can be linearized. By substituting $\sin\theta' \approx x/l$ and $\cos\theta' \approx z/l$ into Eqs. (1) and (2), we can obtain

$$\ddot{x} = \frac{g}{z}x - \frac{J\ddot{\theta}}{mz}. \tag{3}$$

If the energy of the LIPM plus flywheel system is analyzed, the orbital energy (E_{LIP}) can be described by the following Hamilton equation:

$$E_{\mathrm{LIP}} = \frac{1}{2}\dot{x}^2 - \frac{g}{2z}x^2. \tag{4}$$

According to the definition of the CP theory, if the system is in a capture state, its kinetic energy must maintain a constant zero value under a certain joint moment. This value can be substituted into Eq. (4). In this case, the instantaneous capture point (ICP) position (x_{ICP}) of the LIPM plus flywheel system can be expressed as

$$x_{\mathrm{ICP}} = \dot{x}\sqrt{\frac{z}{g}}. \tag{5}$$

For the LIPM plus flywheel system, the position of the ICP can be amended by the speed and position.

In human-exoskeleton systems, the exoskeleton often provides torque to control system movement by means of motors (Lu, 2013; Shafiee-Ashtiani et al., 2017). The pulse torque exerted on the flywheel will affect the step change $\Delta\dot{\theta}$ (that is, $\ddot{\theta}$) of the speed of flywheel, to influence the speed of the system, $\Delta\dot{x} = \frac{J\ddot{\theta}}{mz}$. So, Eq. (5) can be amended as

$$x_{\mathrm{ICP}}^{\mathrm{des}} = \left(\dot{x} - \frac{J\ddot{\theta}}{mz}\right)\sqrt{\frac{z}{g}}. \tag{6}$$

Then, the formula for the target ICP can be obtained. The system can then return to a stable state when it reaches this balance point.

2.2 Stability problem under different gait phases

Through the analysis of the LIPM plus flywheel system, the target ICP can be obtained. However, this solves only the problem of where the target point is. Another key point is when to move forward.

In the CP theory, when an ICP falls into the stability zone (SZ), the system can be considered stable. The stability region is determined by the supporting polygon, in other words, by the bipedal, and changes with the gait phases.

During a single step, the stability area and the point of the ICP both change as the gait phases change. A complete gait can be divided into the following four phases according to the difference of sole pressure

distributions: double support (DS), terminal stance (TS), swing phase (SP), and initial contact (IC) (Wang et al., 2016). The equilibrium characteristics of each phase are shown in Table 1.

Table 1 Stability characteristics of gait phases

Phase	Characteristics
DS	The stability area is composed of a supporting quadrilateral of two legs, and the system is in a relatively stable state
TS	The system gradually changes from a double-support state to a single-support state. It is easy to lose stability due to the lack of lower limb strength and the narrowing of the stability region
SP	The foot is completely off the ground, another lower limb is in a single-support state, and the stability region is determined by the supporting surface of the supporting leg
IC	The system changes from a single-support state or swing state to a double-support state, and then the system returns to balance

DS: double support; TS: terminal stance; SP: swing phase; IC: initial contact

As seen in Fig. 3, the human-exoskeleton system is in a stable state when it is in the DS phase. At the initial stage of swing (the TS phase), the forward leaning of the upper body causes the ICP to move forward, while the stability state narrows because of the movement of the center of gravity, thus leading to instability. In the SP phase, the gait trajectory is amended using the CP theory to estimate the ICP point. Finally, the system returns to a stable state in the IC phase.

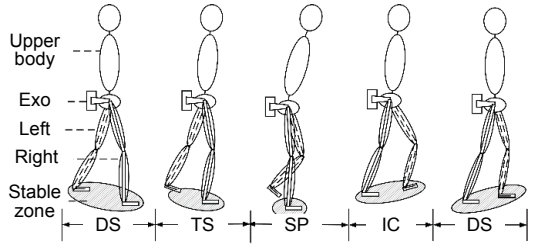

Fig. 3 Stability state changes as gait phase changes

3 Trajectory control of the exoskeleton system

3.1 Trajectory planning based on the CP theory

If the exoskeleton system is simplified to a multi-link system, the position and posture of the i^{th} connecting rod can be represented by $\boldsymbol{p}_i$ and $\boldsymbol{R}_i$ respectively, where $\boldsymbol{p}_i$ is the position vector and $\boldsymbol{R}_i$ is a matrix composed of angles of pitch, roll, and yaw (Masuya and Sugihara, 2015). Then the position and posture formula can be established as

$$\Pi \boldsymbol{T}_i = \Pi \begin{bmatrix} \boldsymbol{R}_i & \boldsymbol{p}_i \\ 0 & 1 \end{bmatrix}. \tag{7}$$

As for the target point (x_{ICP}), which is planned according to the CP theory, the initial angle is $\boldsymbol{\Theta}^0 = \left[\theta_{\text{lh}}^0, \theta_{\text{lk}}^0, \theta_{\text{rh}}^0, \theta_{\text{rk}}^0\right]$. Additionally, the value of $\boldsymbol{\Theta}^{\text{IC}}$ in the IC phase can be calculated by bringing the following equations into the linkage system:

$$\theta_{\text{lk}}^{\text{IC}} = \pi - \arccos\left(\frac{l_{\text{c}}^2 + l_{\text{t}}^2 - x_{\text{p}}^2 - (z_{\text{p}}^0)^2}{2 l_{\text{c}} l_{\text{t}}}\right), \tag{8}$$

$$\theta_{\text{lh}}^{\text{IC}} = -\arctan\left(\frac{x_{\text{p}}}{z_{\text{p}}^0}\right) - \arcsin\left(\frac{l_{\text{c}} \sin\theta_{\text{rk}}}{l_{\text{p}}^{\text{ref}}}\right), \tag{9}$$

$$\theta_{\text{rk}}^{\text{IC}} = \pi - \arccos\left(\frac{l_{\text{c}}^2 + l_{\text{t}}^2 - (x_{\text{p}} - l_{\text{t}})^2 - (z_{\text{p}}^0)^2}{2 l_{\text{c}} l_{\text{t}}}\right), \tag{10}$$

$$\theta_{\text{rh}}^{\text{IC}} = \arctan\left(\frac{x_{\text{p}}}{z_{\text{p}}^0}\right) + \arcsin\left(\frac{l_{\text{c}} \sin\theta_{\text{lk}}}{l_{\text{p}}^{\text{ref}}}\right), \tag{11}$$

where subscripts l and r represent left and right respectively, subscripts k and h represent knee and hip respectively, l_{c} is the calf length, l_{t} is the thigh length, and x_{p}^0 and z_{p}^0 represent the position parameters of the pelvic bone during the IC phase, which can be calculated using θ^0 and other geometric parameters of the exoskeleton system. $x_{\text{p}} = x_{\text{p}}^0 + x_{\text{ICP}}$ is the position parameter of the pelvic bone under the target phase, l_{l} is the set step length of gait planning, $l_{\text{p}}^{\text{ref}} = \sqrt{(x_{\text{p}})^2 + (z_{\text{p}}^0)^2}$ represents the relative distance to point p, and x_{ICP} can be calculated by Eq. (6).

In trajectory planning, the joint trajectory can be programmed with the minimum acceleration, and the fifth-order polynomial can be chosen to do the planning. Taking the hip joint as an example, we have

$$\theta_{\text{h}} = \sum_i a_{\text{h}i} t^i. \tag{12}$$

When the gait parameters ($\boldsymbol{\Theta}^0$ and $\boldsymbol{\Theta}^{\mathrm{IC}}$) and the ratio of the SP phase to the IC phase (λ) have been programmed, the hip joint trajectory can be calculated by

$$\boldsymbol{A}=\begin{bmatrix}\boldsymbol{T}^0\\ \boldsymbol{T}^{\mathrm{IC}}\end{bmatrix}^{-1}\begin{bmatrix}\theta_{\mathrm{h}}^0\\ \omega_{\mathrm{h}}^0\\ 0\\ \theta_{\mathrm{h}}^{\mathrm{IC}}\\ \omega_{\mathrm{h}}^{\mathrm{IC}}\\ 0\end{bmatrix}, \tag{13}$$

$$\boldsymbol{T}=\begin{bmatrix}t^5 & t^4 & t^3 & t^2 & t & 1\\ 5t^4 & 4t^3 & 3t^2 & 2t & 1 & 0\\ 20t^3 & 12t^2 & 6t & 2 & 0 & 0\end{bmatrix}, \tag{14}$$

where $\boldsymbol{A}=[a_{\mathrm{h}5},\ a_{\mathrm{h}4},\ \ldots,\ a_{\mathrm{h}0}]$ can be calculated by Eq. (13). Eq. (14) shows the transfer matrix $\boldsymbol{T}$ and the duration t. Matrix $\boldsymbol{T}^0$ can be calculated by setting $t=t_{\mathrm{s}}$, and matrix $\boldsymbol{T}^{\mathrm{IC}}$ can be calculated when $t=t_{\mathrm{f}}$, where t_{s} and $t_{\mathrm{f}}=t_{\mathrm{s}}+\lambda T_{\mathrm{step}}$ are the start time and end time of the trajectory correction, respectively. θ_{h} and ω_{h} are the angle and angular velocity of the hip joint respectively, which are measured by sensors.

Note that in the calculation of the trajectory of the knee joint, extra consideration should be given to the effect of h_{step}, which is the maximum distance from the ground to the swing leg when the SP is used. Therefore, the planning points should be increased, and the order of the trajectory of the knee joint should be increased.

The final simulation results of the single-step bar are shown in Fig. 4.

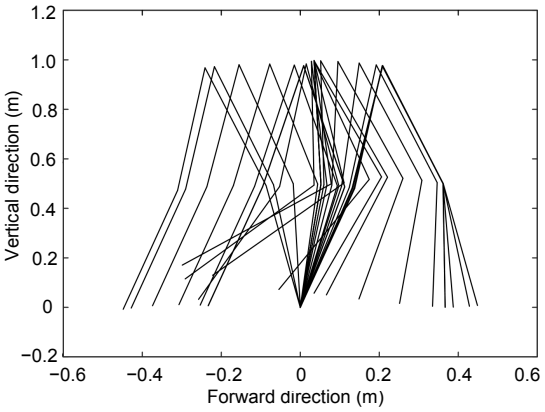

Fig. 4 Bar diagram of a single-step gait

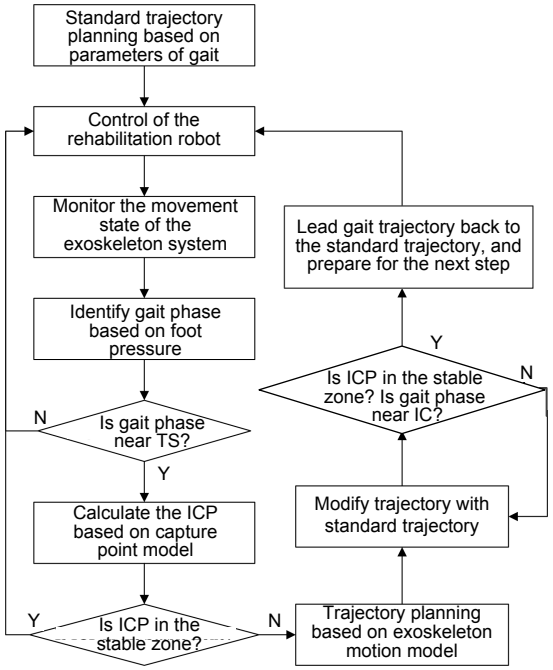

Fig. 5 Control flowchart of the human-exoskeleton system

3.2 Control process of the human-exoskeleton system

A control flowchart of the system is created by combining the analysis of the stability of the human-exoskeleton system in Section 2 and the trajectory planning measures of the exoskeleton in Section 3.1 (Fig. 5).

First, the reference trajectory of the exoskeleton system can be planned through the preset gait parameters. The parameters of movements are monitored by wearable sensors. The sole pressure and joint angle are the major movement parameters. Multi-sensor data is fused to monitor the current motion state and gait phase.

The stability of the system is judged based on the relationship between CP and the stability domain. Without considering the ideal condition of using crutches, the stability domain is formed by supporting polygons in the DS phase. With the gradual transformation from bilateral to unilateral support, the stability domain switches to the supporting surface. When judging the stability, it is necessary to set an appropriate margin.

After judging the occurrence of ability problem of the system, the ICP of the target point and the current motion posture are amended based on the reference trajectory. Finally, the gait phase transforms

into the IC phase, the system returns to stability, and the gait trajectory comes back to the reference trajectory. Otherwise, the system would continue to follow the reference trajectory.

4 Experiments

Experiments were conducted at Zhejiang University. The Zhejiang University Lower Extremity Exoskeleton (ZJULEEX) was used in the experiments (Fig. 6).

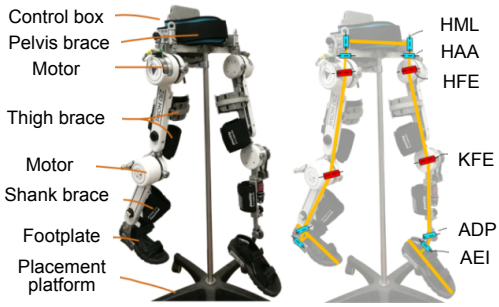

Fig. 6 The Zhejiang University Lower Extremity Exoskeleton (ZJULEEX)
HML: hip medial and lateral rotation; HAA: hip abduction and adduction; HFE: hip flexion/extension; KFE: knee flexion/extension; ADP: ankle dorsiflexion/plantar flexion; AEI: ankle eversion/inversion

ZJULEEX consists of four joint motors, two foot components, two thigh components, two shank components, and a control box on the waist. Each leg of the ZJULEEX has six degrees of freedom, including hip medial and lateral rotation (HML), hip abduction and adduction (HAA), hip flexion/extension (HFE), knee flexion/extension (KFE), ankle dorsiflexion/plantar flexion (ADP), and ankle eversion/inversion (AEI). To simplify the ZJULEEX system, the degrees of freedom of HFE and KFE are driven by joint motors. Other degrees of freedom are limited by spring groups. During walking experiments, ZJULEEX offers a limited motion margin with the help of springs and provides passive adjustment when an external force is applied to the joint.

Five six-axis sensors were used to measure the joint angle of the left knee, left hip, right knee, right hip, and the tilt angle acceleration of the upper body in this system. A pressure sensor was used to measure the sole pressure. Fig. 7 displays the distribution of the measuring points used to judge the current phase and calculate the ZMP.

A hardware communication structure of the ZJULEEX is shown in Fig. 8. Inertial measurement units (IMUs) (Yang et al., 2018) and force sensing resistor units continuously monitored the gait condition and sent the data to the upper computer. The upper computer calculated and predicted the motional intentions of the subject.

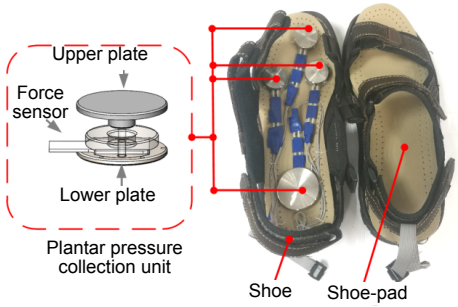

Fig. 7 Pressure measuring system

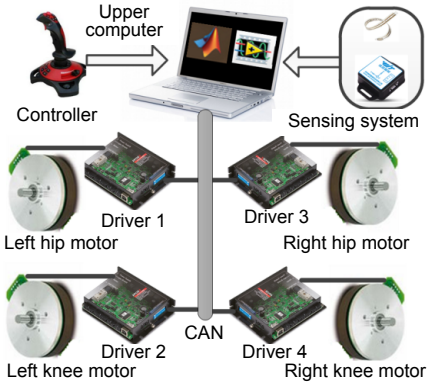

Fig. 8 ZJULEEX hardware communication structure

The test was approved by the Institutional Review Committee of Zhejiang University, and reached agreement with the test subjects. Before the experiments, test subjects were asked to familiarize themselves with the proposed gait to reduce the safety risk of participating in the experiments. To ensure safety, two assistants were present during the experiments to monitor the movements of the test subjects without providing support, and they were able to intervene if necessary.

In the experiments, the volunteers put on the exoskeleton and its measurement system. Measurements of the volunteers are shown in Table 2. As shown in Fig. 9, under the corresponding control measurements, the volunteers walked for a distance of

5 m and repeated this six times. Data from only one side of the exoskeleton was selected to represent the joint angle to simplify the view, because of the similar performance of both sides of the human-exoskeleton system.

Table 2 Measurements of volunteers

Subject	Gender	Height (m)	Weight (kg)
1	Male	1.70	73.0
2	Male	1.71	64.5
3	Male	1.73	57.0
4	Male	1.76	60.0
5	Male	1.72	62.5
6	Male	1.68	65.0
7	Male	1.60	57.5
8	Female	1.67	57.0
9	Female	1.63	53.0
10	Female	1.60	49.0

Fig. 9 Exoskeleton experiment

When following the reference trajectory of the exoskeleton, it was found that the tilt angle and acceleration of the upper body changed frequently. When the right lower limb of the exoskeleton entered the SP and the ZMP increased (moved to the left), the tilt angle of the upper body increased, meaning that the center of gravity of the upper body and the ICP moved forward. The leaning forward of the upper body and the change of the supporting state of the human body from the double-support phase to the single-support phase caused the center of gravity of the human-exoskeleton system to move forward. In addition, the failure of the joint trajectory to respond in time led to early landing of the whole phase and resulted in great fluctuations of the ZMP value. The motion data presented a long average transfer time of the ZMP, the time for the ZMP to shift from the maximum value to the minimum value, and this accounted for about 67% of the gait cycle (Fig. 10).

When running the standard trajectory of the exoskeleton, the CP control strategy was modified in terms of unilateral control, and the lower limb on this side was selected for display. As can be seen in Fig. 11, the relative changes to the leaning angle of the upper body and acceleration were reduced by the corrected trajectory compared with the reference trajectory shown in Fig. 10. Furthermore, the leaning angle of the upper body caused by the change of the center of gravity during the transition from the supporting phase to the SP can be addressed to a certain extent. The range of change for the ZMP was the same as that in Fig. 10, but the transfer process of the ZMP was significantly shorter than that of the former one. This means that the human-exoskeleton system can quickly return to the stable state based on the trajectory control system. In addition, after overbalance of the upper body, the change rates of the joint trajectory and dip acceleration were limited in a small range. It was proved that the corrected trajectory had the same reliability as the original trajectory, and the corrected trajectory guided by the CP theory showed good balance ability during the shift of the center of gravity.

5 Conclusions

In this study, the balance problem of a lower limb rehabilitation exoskeleton has been investigated. The dynamics of the human-exoskeleton system has been analyzed, and the rehabilitation gait has been modified based on the CP theory and gait characteristics. In the process of gait transfer, the unstable problem caused by upper body tilt has been solved. By comparing the difference between the revised and reference trajectories, the motion parameters showed different tendencies. The transfer time of the ZMP has been reduced and the change of dip angle can be dealt with in a short period. This showed that the revised trajectory has better balance ability than the reference trajectory.

In this study, the motion attitude of the TS phase of the human-exoskeleton system has been mainly considered, and the gait trajectory of the subsequent SP has been planned. Therefore, there was a lack of

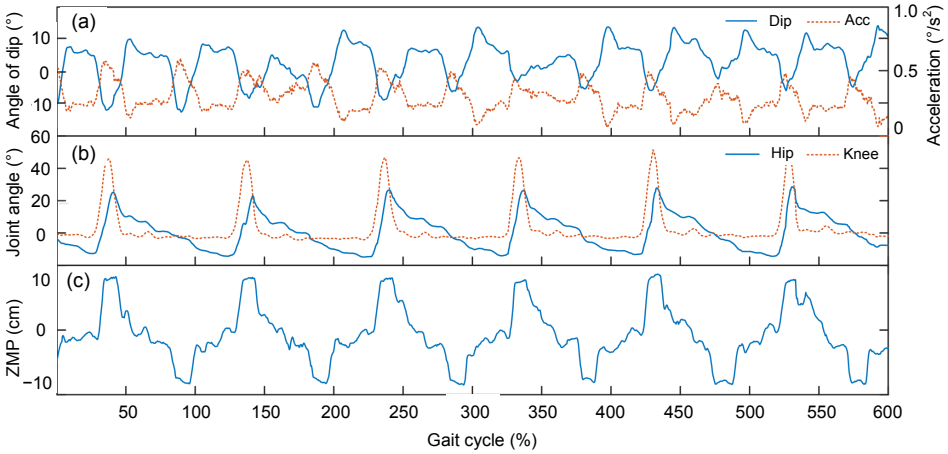

Fig. 10 Gait parameters of the reference trajectory of the human-exoskeleton system: (a) leaning angle, acceleration of the upper body; (b) trajectory of the unilateral hip and knee joint; (c) ZMP trajectory

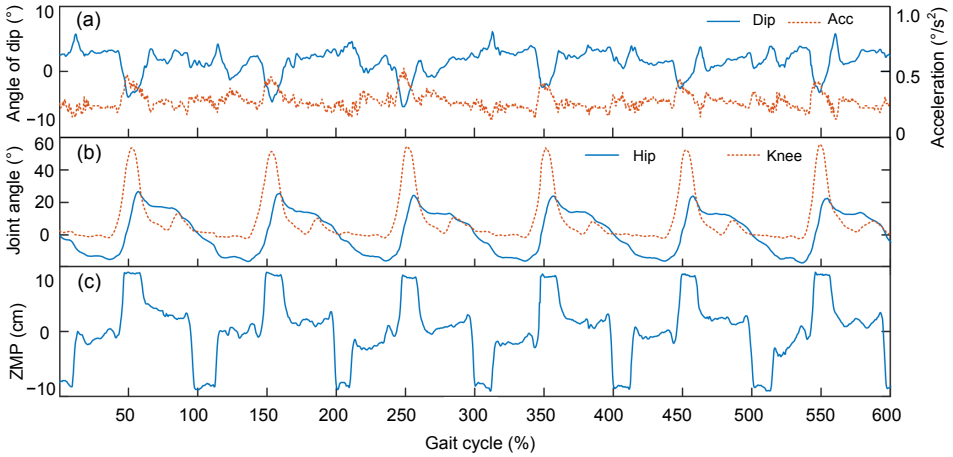

Fig. 11 Modified trajectory gait parameters of the human-exoskeleton system: (a) leaning angle, acceleration of the upper body; (b) trajectory of the unilateral hip and knee joint; (c) ZMP trajectory

ability to cope with the balance problem in other gait phases. However, after gait correction, gait trajectories returned to reference trajectories in the IC phase. In future studies, this processing method will be improved, and the trajectory strategy will be optimized. By constantly modifying and improving the reference trajectory, a more balanced gait trajectory will be obtained as a new reference trajectory.

Compliance with ethics guidelines

Mei-ying DENG, Zhang-yi MA, Ying-nan WANG, Han-song WANG, Yi-bing ZHAO, Qian-xiao WEI, Wei YANG, and Can-jun YANG declare that they have no conflict of interest.

The Ethics Committee of Zhejiang University had reviewed the experimental procedure and method, and approved this experiment. Before the experiment, all subjects signed the informed written consent and agreed to participate in this experiment.

References

Aphiratsakun N, Chairungsarpsook K, Parnichkun M, 2012. ZMP based gait generation of AIT leg exoskeleton—a further gaits generation. *Adv Mater Res*, 488-489:1026-1031. https://doi.org/10.4028/www.scientific.net/AMR.488-489.1026

Englsberger J, Ott C, Roa MA, et al., 2011. Bipedal walking control based on capture point dynamics. IEEE/RSJ Int Conf on Intelligent Robots and Systems, p.4420-4427. https://doi.org/10.1109/IROS.2011.6094435

Jatsun S, Savin S, Yatsun A, 2016. Motion control algorithm for a lower limb exoskeleton based on iterative LQR and ZMP method for trajectory generation. Int Workshop on Medical and Service Robots, p.305-317. https://doi.org/10.1007/978-3-319-59972-4_22

Kawamoto H, Sankai Y, 2005. Power assist method based on phase sequence and muscle force condition for HAL. *Adv Robot*, 19(7):717-734. https://doi.org/10.1163/1568553054455103

Koolen T, de Boer T, Rebula J, et al., 2012. Capturability-

based analysis and control of legged locomotion, part 1: theory and application to three simple gait models. *Int J Robot Res*, 31(9):1094-1113. https://doi.org/10.1177/0278364912452673

Kyeong S, Shin W, Yang M, et al., 2019. Recognition of walking environments and gait period by surface electromyography. *Front Inform Technol Electron Eng*, 20(3): 342-352. https://doi.org/10.1631/FITEE.1800601

Li L, Hoon KH, Tow A, et al., 2015. Design and control of robotic exoskeleton with balance stabilizer mechanism. IEEE/RSJ Int Conf on Intelligent Robots and Systems, p.3817-3823. https://doi.org/10.1109/IROS.2015.7353913

Lu YL, 2013. Research on Balance Control of Humanoid Robot's Standing State. MS Thesis, Northeastern University, China (in Chinese).

Masuya K, Sugihara T, 2015. COM motion estimation of a humanoid robot based on a fusion of dynamics and kinematics information. IEEE/RSJ Int Conf on Intelligent Robots and Systems, p.3975-3980. https://doi.org/10.1109/IROS.2015.7353937

Parietti F, Chan KC, Hunter B, et al., 2016. Design and control of supernumerary robotic limbs for balance augmentation. IEEE Int Conf on Robotics and Automation, p.175-181. https://doi.org/10.1109/ICRA.2015.7139896

Pratt J, Carff J, Drakunov S, et al., 2006. Capture point: a step toward humanoid push recovery. 6th IEEE-RAS Int Conf on Humanoid Robots, p.1-8. https://doi.org/10.1109/ICHR.2006.321385

Shafiee-Ashtiani M, Yousefi-Koma A, Shariat-Panahi M, et al., 2017. Push recovery of a humanoid robot based on model predictive control and capture point. 4th Int Conf on Robotics and Mechatronics, p.1-6. https://doi.org/10.1109/ICRoM.2016.7886777

Strausser KA, Kazerooni H, 2011. The development and testing of a human machine interface for a mobile medical exoskeleton. IEEE/RSJ Int Conf on Intelligent Robots and Systems, p.4911-4916. https://doi.org/10.1109/IROS.2011.6095025

Vukobratović M, Stepanenko J, 1973. Mathematical models of general anthropomorphic systems. *Math Bio-Sci*, 17(3-4): 191-242. https://doi.org/10.1016/0025-5564(73)90071-0

Wang DH, Lee KM, Ji JJ, 2016. A passive gait-based weight-support lower extremity exoskeleton with compliant joints. *IEEE Trans Robot*, 32(4):933-942. https://doi.org/10.1109/TRO.2016.2572692

Wang SQ, Wang LT, Meijneke C, et al., 2015. Design and control of the MINDWALKER exoskeleton. *IEEE Trans Neur Syst Rehabil Eng*, 23(2):277-286. https://doi.org/10.1109/TNSRE.2014.2365697

Yang CJ, Wei QX, Wu X, et al., 2018. Physical extraction and feature fusion for multi-mode signals in a measurement system for patients in rehabilitation exoskeleton. *Sensors*, 18(8):2588. https://doi.org/10.3390/s18082588